DALTON

Crystal structure and spin-doublet electron spin resonance of a magnetically coupled di(μ-phenoxo)-copper(II)nickel(II) complex†

Takanori Aono, Hisae Wada, Yu-ichiro Aratake, Naohide Matsumoto, Hisashi Ōkawa * and Yoshihisa Matsuda

Department of Chemistry, Faculty of Science, Kyushu University, Hakozaki 6-10-1, Higashiku, Fukuoka 812, Japan

The complex $[CuNiL][ClO_4]_2 \cdot H_2O$ ($S_{Ni} = 1$) of a dinucleating macrocycle H_2L, derived from the [2 : 1 : 1] condensation of 2,6-diformyl-4-methylphenol, 1,2-diaminoethane and 1,4-diaminobutane, has been obtained. The efflorescent dimethylformamide (dmf) adduct $[CuNiL][ClO_4]_2 \cdot H_2O \cdot 2dmf$ crystallizes in the orthorhombic crystal system, space group $P2_12_12_1$ with $Z = 4$, $a = 15.62(1)$, $b = 16.49(1)$ and $c = 14.75(1)$ Å. Crystallographic refinement converged with $R = 0.060$ and $R' = 0.048$ for 2958 reflections having $I > 3.00\sigma(I)$. The structure comprises $[CuNiL(dmf)(H_2O)]^{2+}$ where the two metal ions are bridged by the endogenous phenolic oxygens of the macrocycle and Cu ··· Ni is 3.038(2) Å. The Cu resides at a N_2O_2 site with an ethylene lateral chain and assumes an essentially planar geometry, the Ni at a site with a tetramethylene lateral chain and a pseudo-octahedral geometry having dmf and water molecules at the axial sites. The complex $[CuNiL][ClO_4]_2 \cdot H_2O$ exhibits a strong antiferromagnetic spin exchange ($J = -90$ cm^{-1} based on $H = -2JS_1S_2$) and shows an axial ESR feature with $g_{\|} = 2.16$, $g_{\perp} = 2.27$ and $A_{\|} = 64 \times 10^{-4}$ cm^{-1} (in frozen dmf at 78 K), attributable to a spin-doublet ground state. The relations $g_{\perp} > g_{\|}$ and $A_{\|} = -\frac{1}{3}A_{Cu}$ {A_{Cu} is the hyperfine coupling constant of the analogous $[CuZnL][ClO_4]_2 \cdot H_2O$)} demonstrate that one unpaired electron of the spin-coupled complex resides in the molecular orbital of d_{z^2} character comprising d_{z^2}(Cu) and d_{z^2}(Ni).

Heterodinuclear complexes are of interest for their unique physicochemical properties associated with metal–metal interaction and unprecedented functions due to the co-operative effect of dissimilar metal ions.[1–3] Magnetic spin-exchange interactions in such complexes have been extensively studied using cryomagnetic techniques[1,4–6] and these studies have served to elucidate the magnetic spin-exchange mechanism. On the other hand, ESR spectroscopic studies of their electronic structures are very limited because of the difficulty in obtaining well resolved spectra of magnetically condensed complexes.

The simplest case of heterodinuclear complexes with dissimilar spins ($S_1 \neq S_2$) is Cu^{II} ($S_1 = \frac{1}{2}$)–Ni^{II} ($S_2 = 1$).[6–17] In previous ESR studies of copper(II)–nickel(II) complexes no detailed discussion could be made on the electronic nature of the spin-coupled doublet state because of the very poor resolution of the ESR hyperfine structure.[15–17] In the present study such a complex, $[CuNiL][ClO_4]_2 \cdot H_2O$, of a phenol-based dinucleating macrocycle L^{2-} has been obtained and the crystal structure of the dmf (dimethylformamide) adduct, $[CuNiL][ClO_4]_2 \cdot H_2O \cdot 2dmf$, determined by X-ray crystallography.

Experimental

Measurements

Elemental analyses (C, H and N) were obtained at the Elemental Analysis Service Centre of Kyushu University, metal analyses on a Shimadzu AA-610 atomic absorption/flame emission spectrophotometer. Electronic spectra were recorded on a Shimadzu MPS-2000 spectrophotometer in dmf, infrared spectra using a JASCO IR-810 spectrometer with KBr discs. Magnetic susceptibilities of powdered samples were measured on a HOXAN HSM-D SQUID susceptometer in the temperature range 4.2–80 K and on a Faraday balance in the range 80–300 K. Diamagnetic corrections were made using Pascal's constants.[18] X-Band ESR spectra were recorded using a JEOL JEX-FE3X spectrometer on frozen dmf–diglyme (2,5,8-trioxanonane) solutions at liquid-nitrogen temperature.

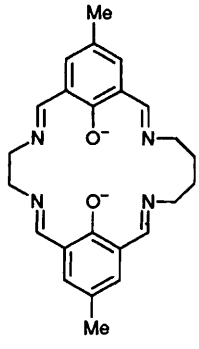

L^{2-}

Preparations

The trinuclear complex, $[Pb(CuL)_2][ClO_4]_2$, was obtained according to our previous paper[19] and used for the preparation of $[CuNiL][ClO_4]_2 \cdot H_2O$ and $[CuZnL][ClO_4]_2 \cdot H_2O$ as reference molecules.

$[CuNiL][ClO_4]_2 \cdot H_2O$. The complex $[Pb(CuL)_2][ClO_4]_2$ (330 mg, 0.25 mmol), nickel(II) sulfate hexahydrate (70 mg, 0.25 mmol) and nickel(II) perchlorate hexahydrate (100 mg, 0.25 mmol) were allowed to react in acetonitrile (30 cm^3) at ambient temperature. The reaction mixture was filtered once to separate the resulting $PbSO_4$ and diffused with diethyl ether to give brown microcrystals. Yield: 86% (Found: C, 39.00; H, 3.80; Cu, 8.30; N, 7.65; Ni, 7.60. Calc. for $C_{24}H_{28}Cl_2CuN_4NiO_{11}$: C, 38.85; H, 3.80; Cu, 8.55; N, 7.55; Ni, 7.90%).

A portion of $[CuNiL][ClO_4]_2 \cdot H_2O$ was recrystallized from dmf to form single crystals of the dmf adduct, $[CuNiL][ClO_4]_2 \cdot H_2O \cdot 2dmf$, suitable for X-ray crystallography (Found:

† *Non-SI units employed:* $\mu_B \approx 9.27 \times 10^{-24}$ J T^{-1}, G = 10^{-4} T.

C, 40.80; H, 4.80; Cu, 7.05; N, 9.45; Ni, 6.65. Calc. for $C_{30}H_{42}Cl_2CuN_6NiO_{13}$: C, 40.60; H, 4.75; Cu, 7.15; N, 9.45; Ni, 6.60%).

[CuZnL][ClO$_4$]$_2$·H$_2$O. This was obtained as greenish brown microcrystals in a way similar to that of [CuNiL][ClO$_4$]$_2$·H$_2$O using zinc(II) sulfate tetrahydrate and zinc(II) perchlorate hexahydrate. Yield: 78% (Found: C, 38.60; H, 3.75; Cu, 8.30; N, 7.50; Zn, 8.80. Calc. for $C_{24}H_{28}Cl_2CuN_4O_{11}Zn$: C, 38.50; H, 3.75; Cu, 8.50; N, 7.50; Zn, 8.75%).

X-Ray structural analysis of [CuNiL][ClO$_4$]$_2$·H$_2$O·2dmf

An efflorescent, prismatic crystal having the approximate dimensions 0.20 × 0.20 × 0.30 mm was sealed in a glass capillary and used for data collection on a Rigaku AFC7R four-circle diffractometer, using graphite-monochromated Mo-Kα radiation and a 12 kW rotating-anode generator at 293 ± 1 K. Cell constants and an orientation matrix for data collection were obtained from 25 reflections in the range 2θ 28.62–30.00°. For the intensity collections the ω–2θ scan mode was used to a maximum 2θ value of 50.0° min^{-1}. Scans of (1.26 + 0.30 tan θ)° were made at a speed of 16.0° min^{-1} in ω. The octant measured was $+h$, $+k$, $+l$ (0–19, 0–20, 0–18). Pertinent crystallographic parameters are summarized in Table 1. A total of 3769 reflections were collected. Three standard reflections were monitored every 150. Over the course of the data collection the standards decreased by 0.1%. A linear correction factor was applied to the data to account for this. The linear absorption coefficient, μ, for Mo-Kα radiation was 12.7 cm^{-1}. Azimuthal scans of several reflections indicated no need for an absorption correction. Reflection data were corrected for Lorentz and polarization effects.

The structure was solved by the direct method and refined by Fourier techniques. The function minimized was $\Sigma w(|F_o| - |F_c|)^2$ with $w = 1/\sigma^2(F_o)$. Non-hydrogen atoms were anisotropically refined. Hydrogen atoms were included in the structure-factor calculations but not refined. The final cycle of full-matrix least-squares refinement was based on 2958 observed reflections with $I > 3.00\sigma(I)$ and 479 variable parameters and converged with $R = 0.060$ and $R' = 0.048$. Neutral atom scattering factors were taken from Cromer and Waber.[20] Anomalous dispersion effects were included in the final calculations;[21] the values for $\Delta f'$ and $\Delta f''$ were taken from ref. 22 and those for the mass-attenuation coefficients from ref. 23. Computations were carried out on an IRIS Indigo computer using the TEXSAN crystallographic package.[24] The final atomic coordinates of the non-hydrogen atoms are given in Table 2.

Complete atomic coordinates, thermal parameters and bond lengths and angles have been deposited at the Cambridge Crystallographic Data Centre. See Instructions for Authors, *J. Chem. Soc., Dalton Trans.*, 1996, Issue 1.

Table 1 Crystallographic data for [CuNiL][ClO$_4$]$_2$·H$_2$O·2dmf

Formula	$C_{30}H_{42}Cl_2CuN_6NiO_{13}$
Colour	Brown
M	887.85
Crystal system	Orthorhombic
Space group	$P2_12_12_1$
a/Å	15.62(1)
b/Å	16.49(1)
c/Å	14.75(1)
U/Å^3	3798(3)
Z	4
D_c/g cm^{-3}	1.553
D_m/g cm^{-3}	1.54
No. of reflections with $\lvert F_o\rvert \geqslant 3\sigma(\lvert F_o\rvert)$	2958
$F(000)$	1836
R^a	0.060
R'^b	0.048

^{a} $\Sigma\lvert\lvert F_o\rvert - \lvert F_c\rvert\rvert/\Sigma\lvert F_o\rvert$. ^{b} $\{[\Sigma w(\lvert F_o\rvert - \lvert F_c\rvert)^2]/\Sigma[w(\lvert F_o\rvert)^2]\}^{\frac{1}{2}}$.

Results and Discussion

Crystal structure of [CuNi(L)][ClO$_4$]$_2$·H$_2$O·2dmf

An ORTEP[25] view of the essential part of the complex is shown in Fig. 1 together with the numbering scheme. Selected bond distances and angles are given in Table 3. The complex cation is $[CuNiL(H_2O)(dmf)]^{2+}$ where the Cu^{II} and Ni^{II} are doubly bridged by the endogenous phenolic oxygens of the macrocycle with the Cu ··· Ni separation 3.038(2) Å. The Cu^{II} resides at the N_2O_2 site of the ethylene lateral chain and assumes an essentially planar geometry. The Cu–N and Cu–O bond lengths range from 1.889(9) to 1.908(7) Å which is normal for planar Cu^{II}. Atoms N(1), N(2), O(1) and O(2) form an approximate plane, their deviations being less than 0.043 Å. The Cu deviates 0.076 Å from this least-squares plane. The ethylene chain assumes the usual skew conformation. The angle between the C(9)–N(1) and C(10)–N(2) bonds with respect to the C(9)–C(10) bond is 32(1)°.

The Ni^{II} resides at the N_2O_2 site of the tetramethylene lateral chain and assumes a pseudo-octahedral geometry, together with dmf and water molecules at the axial sites. The in-plane Ni–N and Ni–O bonds are in the range 2.046(10)–2.073(7) Å, whereas the axial Ni–O(3) (water) and Ni–O(4) (dmf) bonds are slightly elongated [2.101(7) and 2.077(8) Å, respectively]. The Ni–N and Ni–O bonds are significantly longer than the Cu–N and Cu–O bonds, in accord with the high-spin state of the Ni^{II}.[26] Atoms N(3), N(4), O(1) and O(2) form a plane, their deviations being less than 0.018 Å. The deviation of Ni from this least-squares plane is only 0.005 Å. The tetramethylene lateral chain adopts a folded conformation where C(20) and C(23) reside essentially on the basal plane formed by N(3), N(4), O(1) and O(2). Atoms C(21) and C(22) are on the same side with respect to the basal plane and deviate by 0.922 and 0.395 Å, respectively, from the plane.

The complex [CuNiL][ClO$_4$]$_2$·H$_2$O may also contain six-co-ordinate Ni^{II} where the axial donor groups may be a water molecule and a perchlorate ion. This is supported by the split water ν(OH) vibrations at 3525 and 3400 cm^{-1} and split perchlorate ν_3 vibrations in the region 1150–1040 cm^{-1}. The electronic spectrum in dmf shows a distinct band at 541 nm (ε 147 dm^3 mol^{-1} cm^{-1}) attributable to a superposed d–d band of the Cu^{II}.[19] A discernible shoulder near 750 nm ($\varepsilon \approx 10$ dm^3 mol^{-1} cm^{-1}) can be assigned to a d–d component of the six-co-ordinate Ni^{II}. The reference complex [CuZnL][ClO$_4$]$_2$·H$_2$O may have a core structure similar to that of [CuNiL][ClO$_4$]$_2$·H$_2$O, as judged from marked similarity of their IR

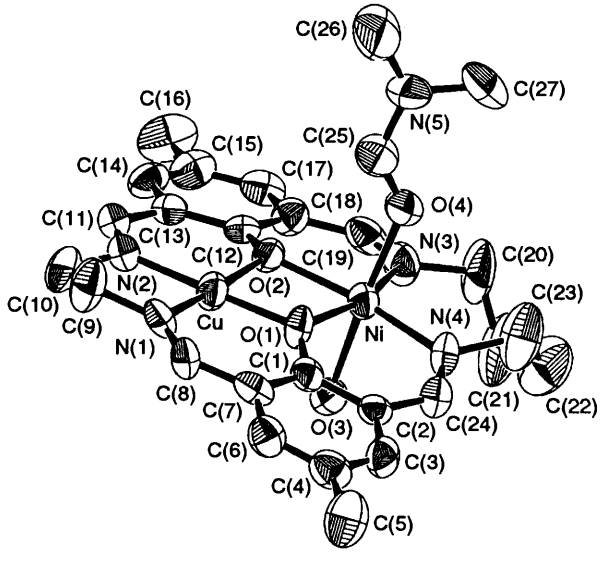

Fig. 1 An ORTEP view of [CuNiL][ClO$_4$]$_2$·H$_2$O·2dmf

Table 2 Final atomic coordinates of $[CuNiL][ClO_4]_2 \cdot H_2O \cdot 2dmf$

Atom	x	y	z	Atom	x	y	z
Cu	0.1971(1)	0.0813(1)	−0.1296(1)	C(5)	0.456(1)	0.180(1)	0.241(1)
Ni	0.0588(1)	0.1186(1)	0.0090(1)	C(6)	0.4033(8)	0.1315(8)	0.0866(8)
Cl(1)	0.2130(3)	0.1545(3)	0.4572(3)	C(7)	0.3394(7)	0.1111(8)	0.0255(8)
Cl(2)	−0.3728(3)	0.0810(3)	−0.1253(3)	C(8)	0.3663(8)	0.0814(8)	−0.0597(8)
O(1)	0.1896(4)	0.1005(4)	−0.0035(5)	C(9)	0.3523(8)	0.029(1)	−0.213(1)
O(2)	0.0751(4)	0.0837(5)	−0.1241(5)	C(10)	0.294(1)	0.0504(8)	−0.287(1)
O(3)	0.0800(5)	0.2396(4)	−0.0297(5)	C(11)	0.1423(8)	0.0569(7)	−0.3107(8)
O(4)	0.0308(5)	0.0018(5)	0.0524(6)	C(12)	0.0239(7)	0.0891(7)	−0.1967(8)
O(5)	0.1898(7)	0.2359(5)	0.8228(6)	C(13)	0.0520(9)	0.0734(7)	−0.2868(8)
O(6)	0.245(1)	0.170(1)	0.5430(8)	C(14)	−0.009(1)	0.0777(8)	−0.3575(8)
O(7)	0.210(1)	0.2240(7)	0.4081(8)	C(15)	−0.094(1)	0.0970(8)	−0.3475(9)
O(8)	0.2706(8)	0.0997(7)	0.417(1)	C(16)	−0.1544(9)	0.0998(9)	−0.425(1)
O(9)	0.1329(8)	0.1215(9)	0.454(1)	C(17)	−0.1194(8)	0.1097(8)	−0.2587(9)
O(10)	−0.417(2)	0.143(1)	−0.132(2)	C(18)	−0.0672(7)	0.1073(7)	−0.1834(8)
O(11)	−0.4250(9)	0.024(1)	−0.142(2)	C(19)	−0.1056(7)	0.1267(9)	−0.0935(9)
O(12)	−0.3207(9)	0.078(2)	−0.185(1)	C(20)	−0.1281(9)	0.146(1)	0.059(1)
O(13)	−0.338(2)	0.079(1)	−0.050(1)	C(21)	−0.099(1)	0.221(1)	0.110(1)
N(1)	0.3179(5)	0.0665(6)	−0.1284(7)	C(22)	−0.061(1)	0.205(1)	0.200(1)
N(2)	0.2064(7)	0.0571(6)	−0.2545(6)	C(23)	0.005(1)	0.140(1)	0.208(1)
N(3)	−0.0695(6)	0.1298(7)	−0.0166(7)	C(24)	0.1505(7)	0.1646(8)	0.1772(8)
N(4)	0.0775(6)	0.1480(6)	0.1430(6)	C(25)	0.0457(9)	−0.0631(8)	0.022(1)
N(5)	0.0066(8)	−0.1322(7)	0.0445(8)	C(26)	0.032(1)	−0.2113(9)	0.013(1)
N(6)	0.1914(8)	0.3426(7)	0.7253(7)	C(27)	−0.057(1)	−0.131(1)	0.115(1)
C(1)	0.2516(7)	0.1234(7)	0.0495(8)	C(28)	0.195(1)	0.2643(7)	0.746(1)
C(2)	0.2317(7)	0.1567(7)	0.1384(8)	C(29)	0.197(1)	0.370(1)	0.633(1)
C(3)	0.300(1)	0.1758(7)	0.1945(8)	C(30)	0.185(1)	0.403(1)	0.796(1)
C(4)	0.3855(8)	0.1623(9)	0.171(1)				

Table 3 Selected bond distances (Å) and angles (°) of $[CuNiL][ClO_4]_2 \cdot H_2O \cdot 2dmf$

Cu–O(1)	1.889(7)	Ni–O(1)	2.073(7)
Cu–O(2)	1.908(7)	Ni–O(2)	2.062(7)
Cu–N(1)	1.902(9)	Ni–N(3)	2.046(10)
Cu–N(2)	1.891(9)	Ni–N(4)	2.056(9)
Ni–O(3)	2.101(7)	Ni–O(4)	2.077(8)
Cu · · · Ni	3.038(2)		
Cu–O(1)–Ni	100.0(3)	Cu–O(2)–Ni	99.8(3)
O(1)–Cu–O(2)	83.8(3)	O(1)–Cu–N(1)	94.2(4)
O(2)–Cu–N(2)	97.0(4)	N(1)–Cu–N(2)	84.6(5)
O(1)–Ni–O(2)	75.7(3)	O(1)–Ni–O(3)	87.5(3)
O(1)–Ni–O(4)	95.8(3)	O(1)–Ni–N(4)	88.8(3)
O(2)–Ni–O(3)	89.3(3)	O(2)–Ni–O(4)	93.4(3)
O(2)–Ni–N(3)	88.3(3)	O(3)–Ni–N(3)	91.1(4)
O(3)–Ni–N(4)	90.8(3)	O(4)–Ni–N(3)	86.2(4)
O(4)–Ni–N(4)	87.3(4)	N(3)–Ni–N(4)	107.2(4)

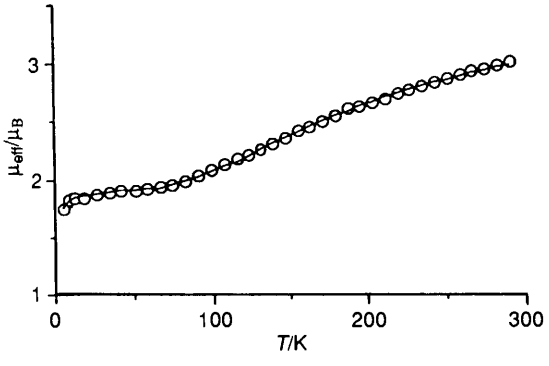

Fig. 2 Temperature dependence of the effective magnetic moment (per CuNi) of $[CuNiL][ClO_4]_2 \cdot H_2O$. The solid curve is based on equation (1) and the parameters $J = -90$ cm^{-1}, $g_{\frac{1}{2}} = 2.17$, $g_{\frac{3}{2}} = 2.13$, $\theta = 0.7$ K and $N_\alpha = 280 \times 10^{-6}$ cm^3 mol^{-1}

spectra. The CuZn complex shows split water ν(OH) vibrations at 3530 and 3400 cm^{-1} and split perchlorate ν_3 vibrations in the region 1130–1040 cm^{-1}.

Cryomagnetic properties of $[CuNiL][ClO_4]_2 \cdot H_2O$

Owing to the highly efflorescent nature of $[CuNiL][ClO_4]_2 \cdot H_2O \cdot 2dmf$, a cryomagnetic study was done for $[CuNiL][ClO_4]_2 \cdot H_2O$ in the temperature range 4.2–300 K. The temperature dependence of the effective magnetic moment is given in Fig. 2. The magnetic moment per CuNi is 2.97 μ_B at room temperature which decreases with decreasing temperature to the near-plateau value of 1.95 μ_B at 80 K. The cryomagnetic behaviour suggests a strong antiferromagnetic interaction between the copper(II) and nickel(II) ions and a thermal population only of the spin-doublet ground state at temperatures lower than 80 K. The slight decrease in magnetic moment below 10 K may be ascribed to an intermolecular magnetic interaction or a zero-field splitting of the nickel(II) ion.[15]

Magnetic analyses were carried out using the magnetic susceptibility expression (1) for ($S_1 = \frac{1}{2}$)–($S_2 = 1$) based on the

$$\chi_m = [N\beta^2/4k(T - \theta)][10g_{\frac{3}{2}}^2 + g_{\frac{1}{2}}^2 \exp(-3J/kT)]/[2 + \exp(-3J/kT)] + N_\alpha \quad (1)$$

isotropic Heisenberg model $H = -2JSS_2$. In this equation $g_{\frac{1}{2}}$ and $g_{\frac{3}{2}}$ are the Zeeman splitting factors associated with the spin-doublet and -quartet states, respectively, and expressed using the local g factors of Cu^{II} and Ni^{II} as $g_{\frac{1}{2}} = (4g_{Ni} - g_{Cu})/3$ and $g_{\frac{3}{2}} = (2g_{Ni} + g_{Cu})/3$.[1,27,28] The θ value is included as the correction term for intermolecular magnetic interaction while other symbols have their usual meanings. The cryomagnetic behaviour can be well reproduced using the parameters $J = -90$ cm^{-1}, $g_{\frac{1}{2}} = 2.17$, $g_{\frac{3}{2}} = 2.13$, $\theta = 0.7$ K and $N_\alpha = 280 \times 10^{-6}$ cm^3 mol^{-1}. The local g factors, g_{Cu} and g_{Ni}, are 2.09 and 2.15, respectively. The discrepancy factor defined as $R(\chi) = [(\Sigma\chi_{obs} - \chi_{calc})^2/(\Sigma\chi_{obs})^2]^{\frac{1}{2}}$ was 9.7×10^{-3}.

The energy separation between the spin-doublet ground state and the spin-quartet excited state is given by $-3J$ (= 270 cm^{-1}) which is large enough to allow thermal population only of the spin-doublet ground state at 80 K. This is in agreement with the observed cryomagnetic behaviour of the complex (Fig. 2).

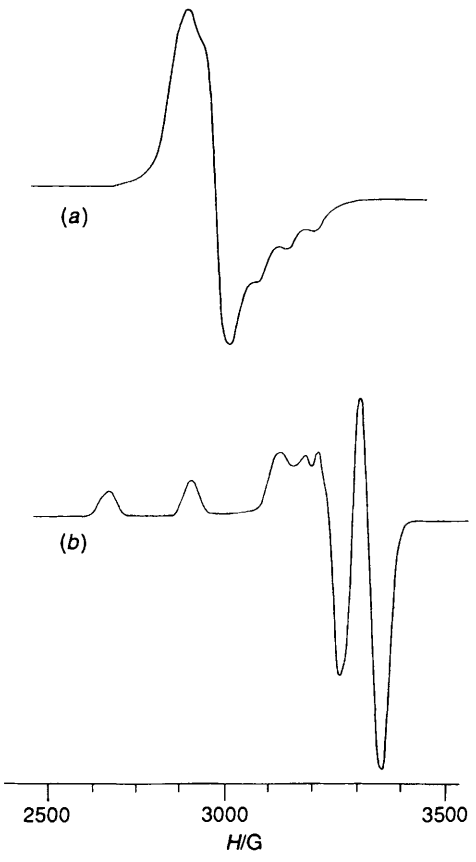

Fig. 3 X-Band ESR spectra of (*a*) $[CuNiL][ClO_4]_2 \cdot H_2O$ and (*b*) $[CuZnL][ClO_4]_2 \cdot H_2O$ (in frozen dmf–diglyme solution at liquid-nitrogen temperature)

ESR Spectra

The X-band ESR spectrum of $[CuNiL][ClO_4]_2 \cdot H_2O$, measured on a frozen dmf–diglyme solution at liquid-nitrogen temperature is given in Fig. 3(*a*). For comparison the ESR spectrum of $[CuZnL][ClO_4]_2 \cdot H_2O$ was determined under the same conditions [Fig. 3(*b*)].

The CuNi complex shows an axial ESR pattern with $g_{\|} = 2.16$ and $g_{\perp} = 2.27$, and on the $g_{\|}$ component is superposed a four-line hyperfine structure ($A_{\|} = 64 \times 10^{-4}$ cm^{-1}) due to the copper nucleus ($I_{Cu} = \frac{3}{2}$). The CuZn complex also shows an axial pattern with $g_{\|} = 2.20$, $g_{\perp} = 2.02$ and $A_{\|} = 189 \times 10^{-4}$ cm^{-1}. The two spectra differ from each other with respect to the relative location of $g_{\|}$ and $g_{\perp}$. The ESR spectrum of the CuZn complex with the relation $g_{\|} > g_{\perp}$ is typical of planar Cu^{II} with one unpaired electron in the $d_{x^2-y^2}$ orbital.[29] The spectrum of the CuNi complex with $g_{\perp} > g_{\|}$ is similar to that of mononuclear Cu^{II} with one unpaired electron in the d_{z^2} orbital.

In the simplest treatment of the magnetic interaction in dinuclear complexes only the singly occupied molecular orbitals of the two magnetic centres are considered. In the $Cu^{II}Ni^{II}$ ($S_{Ni} = 1$) case the overall exchange integral J is given by the mean of two individual exchanges, $J[d_{x^2-y^2}(Cu)–d_{x^2-y^2}(Ni)]$ and $J[d_{x^2-y^2}(Cu)–d_{z^2}(Ni)]$, *i.e* $J = \frac{1}{2}(J_{x^2-y^2,x^2-y^2} + J_{x^2-y^2,z^2})$. It is generally known that the $J_{x^2-y^2,x^2-y^2}$ term is largely negative as demonstrated for dinuclear dicopper(II) complexes.[30,31] The contribution of the $J_{x^2-y^2,z^2}$ term is believed to be weakly antiferromagnetic.[31] Thus, a significant antiferromagnetic interaction is observed in most copper(II)–nickel(II) complexes. As a result of the spin exchange through the $d_{x^2-y^2}(Cu)$–$d_{x^2-y^2}(Ni)$ path there remains one unpaired electron in the d_{z^2} orbital of Ni. However, the ESR spectrum exhibiting the copper hyperfine structure [Fig. 3(*a*)] clearly indicates that the remaining unpaired electron is delocalized on the copper nucleus.

The ESR hyperfine coupling constant in a magnetically coupled M^AM^B system has been derived[27,32,33] and its general expression is given in Kahn's review.[1] The hyperfine structure in the spin-coupled copper(II)–nickel(II) complex is relatively simple because only Cu has isotopes ^{63}Cu (69.1) and ^{65}Cu (30.9%) with $I_{Cu} = \frac{3}{2}$; Ni has isotope ^{61}Ni with $I_{Ni} = \frac{3}{2}$ but its natural abundance is very low (1.25%). According to theory,[27,32,33] the hyperfine coupling constants A'_A and A'_B for a spin-coupled M^AM^B system are given by the local hyperfine coupling constants A_A and A_B as equations (2) and (3) where

$$A'_A = (1 + C)A_A/2 \quad (2)$$

$$A'_B = (1 - C)A_B/2 \quad (3)$$

$C = [S_A(S_A + 1) - S_B(S_B + 1)]/S(S + 1)$. In the Cu^{II} ($S_A = \frac{1}{2}$)–Ni^{II}($S_B = 1$) case, C is $-\frac{5}{3}$ and the hyperfine coupling constant due to the copper nucleus is given by $A'_{Cu} = -A_{Cu}/3$ (the relation $A'_{Ni} = 4A_{Ni}/3$ may hold when the isotope ^{61}Ni is used). If we adopt the hyperfine coupling constant of the CuZn complex (189×10^{-4} cm^{-1}) as the local copper hyperfine constant for the CuNi complex, the observed hyperfine structure (64×10^{-4} cm^{-1}) is indeed one-third that of the CuZn complex. Thus, this study provides the first ESR spectroscopic evidence that one unpaired electron of the spin-coupled CuNi complex resides in the molecular orbital of d_{z^2} character comprising $d_{z^2}(Cu)$ and $d_{z^2}(Ni)$ and is delocalized over the CuNi core.

Acknowledgements

This work was supported by a Grant-in-Aid (No. 07454178) from The Ministry of Education, Science and Culture, Japan. Thanks are also due to Associate Professor T. Isobe for ESR discussion and Mr. M. Ohba for his help with magnetic measurements.

References

1 O. Kahn, *Struct. Bonding (Berlin)*, 1987, **68**, 89.
2 P. Zanello, S. Tamburini, P. A. Vigato and G. A. Mazzocchin, *Coord. Chem. Rev.*, 1987, **77**, 165.
3 P. A. Vigato, S. Tamburini and D. E. Fenton, *Coord. Chem. Rev.*, 1990, **106**, 25.
4 N. Torihara, H. Ōkawa and S. Kida, *Chem. Lett.*, 1978, 1269.
5 O. Kahn, P. Tola and H. Coudanne, *Chem. Phys.*, 1979, **42**, 355; P. Tola, O. Kahn, C. Chauvel and H. Coudanne, *Nouv. J. Chim.*, 1979, **1**, 467; O. Kahn, J. Galy, Y. Journaux, J. Jaud and I. Morgenstern-Badarau, *J. Am. Chem. Soc.*, 1982, **104**, 2165.
6 H. Ōkawa, M. Tanaka and S. Kida, *Chem. Lett.*, 1974, 987; H. Ōkawa, Y. Nishida, M. Tanaka and S. Kida, *Bull. Chem. Soc. Jpn.*, 1977, **50**, 127; N. Torihara, H. Ōkawa and S. Kida, *Inorg. Chim. Acta*, 1976, **26**, 97.
7 C. J. O'Connor, D. P. Freyberg and E. Sinn, *Inorg. Chem.*, 1979, **18**, 1077.
8 R. Graziani, M. Vidali, G. Rizzardi, U. Casellato and P. A. Vigato, *Inorg. Chim. Acta*, 1979, **36**, 145.
9 S. L. Lambert, C. L. Spiro, R. R. Gagne and D. E. Hendrickson, *Inorg. Chem.*, 1982, **21**, 68.
10 R. L. Lintvedt, L. S. Kramer, G. Ranger, P. W. Corfield and M. D. Glick, *Inorg. Chem.*, 1983, **22**, 3580.
11 Y. Journaux, O. Kahn, I. Morgenstern-Badarau, J. Galy, J. Jaud, A. Bencini and D. Gatteschi, *J. Am. Chem. Soc.*, 1985, **107**, 6305.
12 B. Gillon, C. Cavata, P. Schweiss, Y. Journaux, O. Kahn and D. Schneider, *J. Am. Chem. Soc.*, 1989, **111**, 7124.
13 H. Ōkawa, J. Nishio, M. Ohba, M. Tadokoro, N. Matsumoto, M. Koikawa, S. Kida and D. E. Fenton, *Inorg. Chem.*, 1993, **32**, 2949.
14 S. Desjardins, I. Morgenstern-Badarau and O. Kahn, *Inorg. Chem.*, 1984, **23**, 3833.
15 E. Colacio, J. M. Dominguez-Vera, A. Escuer, R. Kivekas and A. Romerosa, *Inorg. Chem.*, 1994, **33**, 3914.
16 I. Morgenstern-Badarau, M. Rerat, O. Kahn, J. Jaud and J. Galy, *Inorg. Chem.*, 1982, **21**, 3050.
17 S. Ohtsuka, M. Kodera, K. Motoda, M. Ohba and H. Okawa, *J. Chem. Soc., Dalton Trans.*, 1995, 2599.

18 E. Boudreaux and L. N. Mulay, *Theory and Application of Molecular Paramagnetism*, Wiley, New York, 1976, pp. 491–495.
19 M. Tadokoro, H. Ōkawa, N. Matsumoto, M. Koikawa and S. Kida, *J. Chem. Soc., Dalton Trans.*, 1991, 1657.
20 D. T. Cromer and J. T. Waber, *International Tables for X-Ray Crystallography*, Kynoch Press, Birmingham, 1974, vol. 4.
21 J. A. Ibers and W. C. Hamilton, *Acta Crystallogr.*, 1964, **17**, 781.
22 D. C. Creagh and W. J. McAuley, *International Tables for X-Ray Crystallography*, ed. A. J. C. Wilson, Kluwer, Boston, 1992, pp. 219–222.
23 D. C. Creagh and H. H. Hubbell, *International Tables for X-Ray Crystallography*, ed. A. J. C. Wilson, Kluwer, Boston, 1992, pp. 200–206.
24 TEXSAN, Molecular Structure Corporation, Houston, TX, 1985.
25 C. K. Johnson, ORTEP, Report 3794, Oak Ridge National Laboratory, Oak Ridge, TN, 1965.
26 R. D. Shannon, *Acta Crystallogr., Sect. A*, 1976, **32**, 751.
27 C. C. Chao, *J. Magn. Reson.*, 1973, **10**, 1.
28 R. P. Scaringe, D. J. Hodgson and W. E. Hatfield, *Mol. Phys.*, 1978, **35**, 701.
29 B. A. Goodman and J. B. Raynor, *Adv. Inorg. Chem. Radiochem.*, 1970, **13**, 135.
30 M. Melnik, *Coord. Chem. Rev.*, 1982, **42**, 259.
31 C. J. Cairns and D. H. Busch, *Coord. Chem. Rev.*, 1986, **69**, 1.
32 E. Buluggiu, *J. Phys. Chem. Solids*, 1980, **41**, 1175.
33 R. P. Scaringe, D. Hodgson and W. E. Hatfield, *Mol. Phys.*, 1978, **35**, 701.

Received 17*th July* 1995; *Paper* 5/04656D